Available online at www.sciencedirect.com
ScienceDirect
Journal of Computational and Applied Mathematics 210 (2007) 71 – 77
JOURNAL OF COMPUTATIONAL AND APPLIED MATHEMATICS
www.elsevier.com/locate/cam

Numerical algorithms for simulations of a traffic model on road networks

G. Bretti[a,*], R. Natalini[b], B. Piccoli[b]

[a] Department of Information Engineering and Applied Mathematics of the University of Salerno, via Ponte don Melillo, 84084 Fisciano (SA), Italy
[b] Istituto per le Applicazioni del Calcolo "M. Picone", Viale del Policlinico 137, 00161 Roma, Italy

Received 20 July 2005; received in revised form 30 January 2006

Abstract

We introduce a simulation algorithm based on a fluid-dynamic model for traffic flows on road networks, which are considered as graphs composed by arcs that meet at some junctions. The approximation of scalar conservation laws along arcs is made by three velocities Kinetic schemes with suitable boundary conditions at junctions. Here we describe the algorithm and we give an example.

MSC: 65M06; 90B20; 90B10; 35L65; 34B45

Keywords: Scalar conservation laws; Traffic flow; Fluid-dynamic models; Finite difference schemes; Boundary conditions

1. Introduction

The comprehension of traffic behaviour in urban context is the principal aim in the study of traffic problems. This analysis is mainly focused on the maximization of cars flow, and the minimization of traffic congestions, accidents and pollution. In general, network models of transportation systems are assumed to be static, but these models do not allow a correct simulation of heavily congested urban road networks. For this reason, traffic engineers started to consider some alternative models, often referred to as **DTA** (dynamic traffic assignment) or *within-day* models, see the review paper [2] and references therein. Within-day modelling is characterized by the reproduction of the traffic flow motion on the network. However, the main problems are of two type: these models do not properly reproduce the backward propagation of shocks and there is a difficulty of collecting experimental data.

On the other hand, microscopic models are sensitive to small perturbations and it can be difficult to give a qualitative description and visualization of phenomena on a macroscopic scale.

Here we deal with the fluid-dynamic models proposed in [5,6], which are macroscopic models with some traffic regulation strategies (within-day models). In the 1950s James Lighthill and Gerald Whitham in [8], and independently Richards in [10], proposed to apply fluid-dynamics concepts to traffic. In a single road, this non-linear model is based on the conservation of cars:

$$\partial_t \rho + \partial_x f(\rho) = 0, \tag{1}$$

* Corresponding author.
E-mail addresses: g.bretti@iac.cnr.it (G. Bretti), r.natalini@iac.cnr.it (R. Natalini), b.piccoli@iac.cnr.it (B. Piccoli).

0377-0427/$ - see front matter
doi:10.1016/j.cam.2006.10.057

where $\rho=\rho(t,x)\in[0,\rho_{\max}]$ is the density of cars, $(t,x)\in\mathbf{R}^2$ and $f(\rho)$ is the flux. Fluid-dynamic models can describe macroscopic phenomena as shocks formation and propagation. Since they can develop discontinuities in a finite time even starting from smooth initial data, a great consideration of analytical and numerical aspects is needed. Note that, in all classical works on traffic flows, only a single road was taken into account. More recently, in [5,6], some models have been proposed for traffic flow on road networks connected by junctions. Junctions play a key-role: problem is underdetermined even imposing the conservation of cars. Thus we need to make some assumptions to ensure existence and uniqueness.

The case where the number of incoming roads is greater than the number of outgoing ones, is not covered in general by the analysis of [6]. In the case of two incoming and one outgoing roads a loss of uniqueness for the solutions occurs, due to the fact that if not all cars can go through the junction then there should be a yielding rule between incoming roads. Hence, we introduce a new parameter $q\in]0,1[$, the *right of way* (see [5]), which represents, among cars passing through junctions, the percentage of cars coming from the first road. The main contribution is represented by the introduction of suitable boundary conditions at junctions for numerical schemes [3]. In particular, using kinetic approximation methods adapted the considered problem we get quite stable solutions. Some numerical experiments show the effectiveness of our approximation.

2. Backgrounds

The conservation of cars is described by the equation [8,10]

$$\partial_t\rho+\partial_x f(\rho)=0, \tag{2}$$

where $\rho=\rho(t,x)$ is the density of cars, with $\rho\in[0,\rho_{\max}]$, $(t,x)\in\mathbf{R}^2$ and $\rho_{\max}$ is the maximum density of cars on the road; $f(\rho)$ Is The flux, which can be written $f(\rho)=\rho v(\rho)$, with v the average velocity, typically a smooth decreasing function of ρ. For Eq. (2) on $\mathbf{R}$ there exists a unique weak entropy solution for every initial data in L^∞.

A road network is a finite number of roads modelled by intervals $[a_i,b_i]$ that meet at some junctions. We give boundary data and solve associated boundary problems for the endpoints (not infinite) that do not meet at any junction. System at a junction is underdetermined even imposing the conservation of cars, expressed by the Rankine–Hugoniot condition:

$$\sum_{i=1}^{n} f(\rho_i(t,b_i))=\sum_{j=n+1}^{n+m} f(\rho_j(t,a_j)),$$

where ρ_i, $i=1,\ldots,n$, and ρ_j, $j=n+1,\ldots,n+m$, are the car densities, respectively, on incoming and outgoing roads. To uniquely solve Riemann problems at junctions we make the following assumptions:

(A) there are some fixed coefficients, the prescribed preferences of drivers, expressing the distribution of traffic from incoming to outgoing roads;
(B) respecting (A), drivers behave in order to maximize the flux through junctions.

To deal with rule (A) we fix a matrix, called *traffic distribution matrix*:

$$A=\{\alpha_{ji}\}_{j=n+1,\ldots,n+m,i=1,\ldots,n\in\mathbf{R}^{m\times n}}\quad \text{with } 0<\alpha_{ji}<1,\quad \sum_{j=n+1}^{n+m}\alpha_{ji}=1$$

for $i=1,\ldots,n$ and $j=n+1,\ldots,n+m$, where α_{ji} is the percentage of drivers arriving from the ith incoming road that take the jth outgoing road.

In [6] it was proved existence of each solution to Cauchy problems respecting rules (A) and (B). In the case $m<n$ it is necessary to introduce a further rule, see [5]. In particular, when $m=1$, $n=2$ we fix a new *right of way* parameter $q\in]0,1[$ and assign the rule:

(C) not all cars can enter the outgoing road and C is the quantity that can do it. Then qC cars come from first incoming road and $(1-q)C$ cars from the second.

The rule (C) allows us to uniquely solve Riemann problems.

Assuming that the flux is a smooth, strictly concave function there exists a unique admissible solutions for the Riemann problem at a junction, see [6]. Now we describe the construction of solutions (see [6]). We use initial data at the endpoints to determine new states at junctions in such a way that the waves emerge out of junctions. Thus we get sets of maximization region and we can compute the maximum incoming fluxes $\hat{\gamma}_i$ for $i \in \{1, \dots, n\}$ satisfying rule (B). Then the corresponding densities $\hat{\rho}_i \in [0, 1]$ are derived. Recalling rule (A) we obtain $\hat{\gamma}_j \doteq \sum_{i=1}^{n} \alpha_{ji}\hat{\gamma}_i$, $j = n+1, \dots, n+m$, and determine $\hat{\rho}_j \in [0, 1]$. Since $(\hat{\gamma}_1, \dots, \hat{\gamma}_n) \in \Omega$, $\hat{\rho}_j$ exists and is unique for every $j \in \{n+1, \dots, n+m\}$. The weak solution on each road is given by the solution to Riemann problem with data $(\rho_{i0}, \hat{\rho}_i)$ for incoming roads and $(\hat{\rho}_j, \rho_{j0})$ for outgoing roads. The solution can be, respectively, a shock or a rarefaction. As the speed of propagation is finite, following [6] we can build a sequence of solutions to Cauchy problems via a wave front tracking algorithm. Admissible solutions are obtained solving $(\rho_{i0}, \hat{\rho}_i)$ by waves with negative speed and $(\hat{\rho}_j, \rho_{j0})$ by waves with positive speed.

3. Numerical approximation

For definitiveness, we choose the following flux function, due to Greenshields (see [7])

$$f(\rho) = v_{\max}\rho\left(1 - \frac{\rho}{\rho_{\max}}\right). \tag{3}$$

Without loss of generality, we can set for simplicity $\rho_{\max} = 1 = v_{\max}$, so that $f(\rho) = \rho(1-\rho)$, with a unique maximum $\sigma = \frac{1}{2}$. We define a numerical grid in $\mathbf{R}^N \times (0, T)$ where Δx is the space step, Δt the time step and $(x_m, t_n) = (m\Delta x, n\Delta t)$ grid points, $m \in \mathbf{Z}$, $n \in \mathbf{N}$.

3.1. Kinetic method for a boundary value problem [1]

Consider the initial-boundary value conservation equations

$$\rho_t + F(\rho)_x = 0, \tag{4}$$
$$\rho(x, 0) = \rho_0(x), \quad x \geqslant 0, \tag{5}$$
$$\rho(0, t) = \rho_b(t), \quad t \geqslant 0. \tag{6}$$

We have $\rho(x, t) \in \mathbf{R}$ for $x \geqslant 0$, $t \geqslant 0$, and F is a Lipschitz continuous function. A kinetic approximation of the problem (4) is obtained solving the following BGK-like system of N non-linear equations

$$\partial_t f_k^\varepsilon + \lambda_k \partial_x f_k^\varepsilon = \frac{1}{\varepsilon}(M_k(\rho^\varepsilon) - f_k^\varepsilon), \tag{7}$$

where λ_k are fixed velocities (a set of real numbers not all zero), ε is a positive parameter, and each f_k^ε is a function of $\mathbf{R}^+ \times [0, T]$ with values in $\mathbf{R}$. We impose the corresponding initial and boundary data:

$$f_k^\varepsilon(x, 0) = M_k(\rho_0(x)), \quad x \in \mathbf{R}^+, \qquad f_k^\varepsilon(0, t) = M_k(\rho_b(t)), \quad \forall \lambda_k > 0, \quad t \geqslant 0. \tag{8}$$

Functions M_k, $k = 1, \dots, N$, are the Maxwellian functions depending on u^ε, F and λ_i. To have the convergence of $\rho^\varepsilon = \sum_{k=1}^{N} f_k^\varepsilon$ when $\varepsilon \to 0$ towards the solution of the problem (4), we need to impose the following compatibility conditions:

$$\sum_{k=1}^{N} M_k(\rho) = \rho, \quad \sum_{k=1}^{N} \lambda_k M_k(\rho) = F(\rho), \tag{9}$$

showing the link between problem (4) and system (7). A sufficient condition for convergence is that M is monotone non-decreasing on I, [9]. Then the following subcharacteristic condition is satisfied for all $\rho \in I$:

$$\min_k \lambda_k \leqslant F'(\rho) \leqslant \max_k \lambda_k. \tag{10}$$

3.1.1. Kinetic approximations [9]

3.1.1.1. Three velocities model. Dealing with more velocities corresponds to more accurate approximation schemes. Take $N=3$ and the velocities $\lambda_3=-\lambda_1=\lambda>0$, $\lambda_2=0$. The approximated kinetic system has the Maxwellian functions given by

$$M_1(\rho)=\frac{1}{\lambda}\begin{cases}0 & \text{if } \rho\leqslant\frac{1}{2},\\ \rho(\rho-1)+\frac{1}{4} & \text{if } \rho\geqslant\frac{1}{2},\end{cases}\quad M_3(\rho)=\frac{1}{\lambda}\begin{cases}\rho(1-\rho) & \text{if } \rho\leqslant\frac{1}{2},\\ \frac{1}{4} & \text{if } \rho\geqslant\frac{1}{2},\end{cases}$$
$$M_2(\rho)=\begin{cases}\left(1-\frac{1}{\lambda}\right)\rho+\frac{1}{\lambda}\rho^2 & \text{if } \rho\leqslant\frac{1}{2},\\ \left(1+\frac{1}{\lambda}\right)\rho-\frac{1}{\lambda}\rho^2-\frac{1}{2\lambda} & \text{if } \rho\geqslant\frac{1}{2}.\end{cases}$$

At the boundary we impose $f_3(0,t)=M_3(\rho_b(t))$ and assume that the Maxwellian functions are MND.

3.1.2. Numerical scheme

Following [1] we obtain a numerical scheme for the initial boundary value problem (4)–(6). As usual, we discretize data of the problem by a piecewise constant approximation and we take for $k=1,2,3$

$$f^n_{-1,k}=M_k(\rho^n_b),\quad 0\leqslant n\leqslant M-1,\quad f^0_{m,k}=M_k(\rho^0_m),\ \ m\in\mathbf{N}. \tag{11}$$

The scheme written in the Harten formulation including both first and second order in space approximation reads

$$m\geqslant 0,\ \begin{cases} f^{n+1/2}_{m,k}=f^n_{m,k}(1-D^n_{m-1/2,k})+D^n_{m-1/2,k}f^n_{m-1,k} & \text{if } \lambda_k>0,\\ f^{n+1/2}_{m,k}=f^n_{m,k}(1-D^n_{m+1/2,k})+D^n_{m+1/2,k}f^n_{m+1,k}, & \text{if } \lambda_k\leqslant 0,\end{cases} \tag{12}$$

where the expression of functions $D^n_{m,k}$ determine a scheme, respectively, of first or second order

$$D^n_{m+1/2,k}=\xi_k=|\lambda_k|\frac{\Delta t}{\Delta x},\ \ D^n_{m+1/2,k}=\xi_k\left(1+\operatorname{sgn}(\lambda_k)\Delta x\frac{(1-\xi_k)}{2}\frac{(\delta^n_{m+1,k}-\delta^n_{m,k})}{\Delta f^n_{m+1/2,k}}\right),$$

and $\delta^n_{m,k}$ represent limited slopes

$$\delta^n_{m,k}=\operatorname{minmod}\left(\frac{\Delta f^n_{m+1/2,k}}{\Delta x},\frac{\Delta f^n_{m-1/2,k}}{\Delta x}\right),$$

with $\Delta f^n_{m+1/2,k}=f^n_{m+1,k}-f^n_{m,k}$ and $\operatorname{minmod}(a,b)=\min(|a|,|b|)\operatorname{sgn}(a)+\operatorname{sgn}(b)/2$. If $\Delta f^n_{m+1/2,k}=0$, we set $D^n_{m+1/2,k}=\xi_k$. It is necessary to assign the boundary value $f^n_{b,k}=f^n_{-1,k}$ only for positive velocities. Note that if $\lambda_k>0$, $D^n_{m+1/2,k}$ is defined for $m\geqslant -1$, in the other cases is available for $m\geqslant 0$. For the convergence results see [1]. The time step restriction for both cases is

$$\max_{1\leqslant k\leqslant N}|\lambda_k|\Delta t\leqslant\Delta x. \tag{13}$$

Under the compatibility conditions (9) we find the exact solution of the system and the identity holds $\rho^{n+1}_m=\sum_k f^{n+1/2}_{m,k}=\rho^{n+1/2}_m$.

3.2. Boundary conditions and conditions at junctions

3.2.1. Boundary conditions

For $m=0$ we take for the boundary $\delta^n_{-1,k}=0$. In this case, the slope $\delta^n_{0,k}$ can be defined as

$$\delta^n_{0,k}=\operatorname{minmod}\left(\frac{f^n_{1,k}-f^n_{0,k}}{\Delta x},2\frac{f^n_{0,k}-M_k(\rho^n_b)}{\Delta x}\right),\quad \lambda_k>0,\qquad \delta^n_{0,k}=\frac{f^n_{1,k}-f^n_{0,k}}{\Delta x},\quad \lambda_k<0.$$

When $m=N$ the scheme for $\lambda_k<0$ requires the values $f^n_{N+1,k}$, $f^n_{N+2,k}$, that can be obtained, for instance, by imposing a Neumann condition.

3.2.2. Conditions at a junction

At the right boundary ($m = N$) of roads linked to the junction on the right, we need $f^n_{N+1,k} = M_k(f^{-1}(\hat{\gamma}_i))$ for $\lambda_k < 0$. Moreover we use the Neumann condition $f^n_{N+2,k} = f^n_{N+1,k}$ for roads not linked on the right. At the left boundary ($m = 0$) of roads linked on the left endpoint, if $\lambda_k > 0$ we need the value $f^n_{-1,k} = M_k(f^{-1}(\hat{\gamma}_j))$. Note that $\hat{\gamma}_i, \hat{\gamma}_j$ are the maximized incoming and outgoing fluxes described in Section 2, where densities are recovered respecting the claim that waves emerge out of junctions. For instance, for incoming roads, $i = 1, 2$, we have:

- if $\rho^n_N \in [0, \sigma]$ and $\hat{\gamma}_i < F(\rho^n_N)$ then $F^{-1}(\hat{\gamma}_i) \in [\tau(\rho^n_N), 1)$,
- if $\rho^n_N \in [0, \sigma]$ and $\hat{\gamma}_i = F(\rho^n_N)$ then $F^{-1}(\hat{\gamma}_i) = \rho^n_N$,
- if $\rho^n_N \in [\sigma, 1]$ then $F^{-1}(\hat{\gamma}_i) \in [\sigma, 1]$.

4. Tests

Here we present some numerical tests performed by the three-velocities Kinetic schemes of first ($3VK_1$) and second ($3VK_2$) order with $\lambda_3 = -\lambda_1 = 1.0$ and $\lambda_2 = 0$. We introduce the formal numerical order γ of a numerical method as an average in the following way:

$$\gamma = \frac{1}{S} \sum_{s=1}^{S} \gamma_s \quad \text{with } \gamma_s = \log_2 \left(\frac{\mathrm{e}^s(1)}{\mathrm{e}^s(2)} \right), \quad s = 1, \ldots, S \tag{14}$$

and s the index of roads composing the network. The L^1-error on each road is

$$\mathrm{e}^s(p) = \frac{\Delta x}{p} \sum_{l=0,\ldots,pL} \left| w_l^{pM}\left(\frac{\Delta x}{p}\right) - w_{2l}^{pM}\left(\frac{\Delta x}{2p}\right) \right|, \quad p = 1, 2, \quad s = 1, \ldots, S, \tag{15}$$

where $w^M_m(\Delta x)$ denotes the numerical solution obtained with the space step discretization equal to Δx, computed in x_m at the final time $t_M = T$.

4.1. Two incoming-two outgoing roads

Let us fix the traffic distribution matrix

$$A = \begin{pmatrix} 0.4 & 0.3 \\ 0.6 & 0.7 \end{pmatrix} \tag{16}$$

and consider constant initial and boundary data

$$\begin{aligned} &\rho_1(0,x) = \rho_4(0,x) = \sigma, \quad \rho_2(0,x) = \rho_3(0,x) = f^{-1}\left(\frac{\alpha_1}{1-\alpha_2} f(\sigma)\right) \sim 0.83, \\ &\rho_{1,b}(0,t) = \sigma, \quad \rho_{2,b}(0,t) = f^{-1}\left(\frac{\alpha_1}{1-\alpha_2} f(\sigma)\right). \end{aligned} \tag{17}$$

Then we introduce a perturbation on road 1, setting initial datum as follows:

$$\rho_1(0,x) = \begin{cases} \sigma & \text{if } 0 \leqslant x \leqslant 0.5, \\ 0.4 & \text{if } x \geqslant 0.5. \end{cases} \tag{18}$$

Initial and boundary data on other roads are taken as in (17). After a certain time ($t \sim 8$) the wave $(\rho_1, \rho_{1,0})$ interacts with the junction thus determining a shock wave travelling on road 3. At time $T = 470$ a new equilibrium configuration is reached. In Figs. 1 and 2 we describe the evolution in time of road 1 and road 3, where numerical solutions are produced by the $3VK_2$ scheme. For further details see [3].

In the following Tables 1 and 2 are reported orders and L^1-errors, defined by (14) and (15), of $3VK_1$ and $3VK_2$ schemes, respectively, before and after interactions at the junction. Here we used $3VK_2$ scheme with boundary condition $\sigma^n_{0,k} = 0$ for $\lambda_k < 0$.

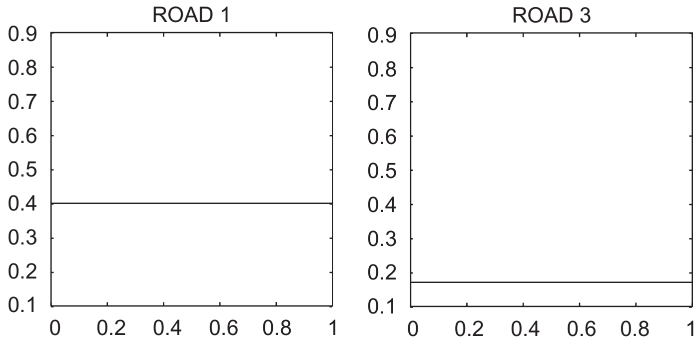

Fig. 1. Situation after the interaction, $T = 25$, $h = 0.025$.

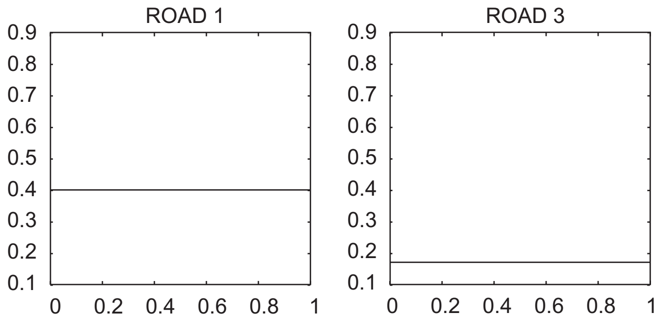

Fig. 2. Final configuration, $T = 470$, $h = 0.025$.

Table 1
Convergence order γ and errors of 3-velocities kinetic schemes of first ($3VK_1$) and second ($3VK_2$) order, for $T = 1$

h	$3VK_1$		$3VK_2$	
	γ	L^1-error	γ	L^1-error
0.2	1.4	6.00949e − 003	1.9	6.72896e − 003
0.1	0.88	2.27511e − 003	0.94	1.82122e − 003
0.05	0.93	1.23605e − 003	0.98	9.49608e − 004
0.025	0.98	6.48354e − 004	0.99	4.81271e − 004
0.0125	0.99	3.29293e − 004	0.99	2.41161e − 004
0.00625	1.0	1.65002e − 004	1.0	1.20602e − 004

Table 2
L^1-errors of 3-velocities kinetic schemes of first ($3VK_1$) and second ($3VK_2$) order in comparison with the exact solution at time $T = 20$

h	$3VK_1$	$3VK_2$
	L^1-error	L^1-error
0.2	5.58553e − 002	5.53875e − 002
0.1	2.24683e − 002	2.07874e − 002
0.05	9.74289e − 003	6.93735e − 003
0.025	5.76965e − 003	5.41827e − 003
0.0125	8.02476e − 003	8.04770e − 003
0.00625	5.62481e − 003	5.63628e − 003

5. Conclusions

An elaboration and an implementation of a numerical algorithm provided approximated solutions to the presented problem (for animations see [4]). Since along roads the approximation works as for conservation laws, the new and original aspect is the treatment of the solution at junctions.

Acknowledgement

The authors would like to thank Antonino Sgalambro for his assistance with the computational work.

References

[1] D. Aregba-Driollet, V. Milišić, Kinetic approximation of a boundary value problem for conservation laws, Numer. Math. 97 (2004) 595–633.
[2] V. Astarita, Node and link models for network traffic flow simulation, Math. Comput. Model. 35 (2002) 643–656.
[3] G. Bretti, R. Natalini, B. Piccoli, Numerical approximations of a traffic flow model on networks, Networks and Heterogeneous Media 1 (2006) 57–84.
[4] G. Bretti, A. Sgalambro, ⟨http://www.iac.rm.cnr.it/ bretti/TrafficNumericalSolution.html⟩.
[5] Y. Chitour, B. Piccoli, Traffic circles and timing of traffic lights for cars flow, Discrete Continuous Dynam. Systems—Ser. B 5 (2005) 599–630.
[6] G.M. Coclite, M. Garavello, B. Piccoli, Traffic flow on a road network, SIAM Math. Anal. 36 (2005) 1862–1886.
[7] B.D. Greenshields, A study in highway capacity, Highway Res. Board Proc. 14 (1935) 448–477.
[8] M.J. Lighthill, G.B. Whitham, On kinematic waves I and II. A theory of traffic flow on long crowded roads, Proc. Roy. Soc. London. Ser. A. 229 (1955).
[9] R. Natalini, A discrete kinetic approximation of entropy solutions to multidimensional scalar conservation laws, J. Differential Equations 148 (1998) 292–317.
[10] P.I. Richards, Shock waves on the highway, Oper. Res. 4 (1956) 42–51.